TFTR PLASMA REGIMES

R.J. HAWRYLUK, V. ARUNASALAM, M.G. BELL, M. BITTER, W.R. BLANCHARD, N.L. BRETZ, R. BUDNY, C.E. BUSH[1], J.D. CALLEN[2], S.A. COHEN, S.K. COMBS[1], S.L. DAVIS, D.L. DIMOCK, H.F. DYLLA, P.C. EFTHIMION, L.C. EMERSON[1], A.C. ENGLAND[1], H.P. EUBANK, R.J. FONCK, E. FREDRICKSON, H.P. FURTH, G. GAMMEL, R.J. GOLDSTON, B. GREK, L.R. GRISHAM, G. HAMMETT, W.W. HEIDBRINK[3], H.W. HENDEL[4], K.W. HILL, E. HINNOV, S. HIROE[1], H. HSUAN, R.A. HULSE, K.P. JAEHNIG, D. JASSBY, F.C. JOBES, D.W. JOHNSON, L.C. JOHNSON, R. KAITA, R. KAMPERSCHROER, S.M. KAYE, S.J. KILPATRICK, R.J. KNIZE, H. KUGEL, P.H. LaMARCHE, B. LeBLANC, R. LITTLE, C.H. MA[1], D.M. MANOS, D.K. MANSFIELD, R.T. McCANN, M.P. McCARTHY, D.C. McCUNE, K. McGUIRE, D.H. McNEILL, D.M. MEADE, S.S. MEDLEY, D.R. MIKKELSEN, S.L. MILORA[1], W. MORRIS[5], D. MUELLER, V. MUKHOVATOV[6], E.B. NIESCHMIDT[7], J. O'ROURKE[8], D.K. OWENS, H. PARK, N. POMPHREY, B. PRICHARD, A.T. RAMSEY, M.H. REDI, A.L. ROQUEMORE, P.H. RUTHERFORD, N.R. SAUTHOFF, G. SCHILLING, J. SCHIVELL, G.L. SCHMIDT, S.D. SCOTT, S. SESNIC, J.C. SINNIS, F.J. STAUFFER[9], B.C. STRATTON, G.D. TAIT, G. TAYLOR, J.R. TIMBERLAKE, H.H. TOWNER, M. ULRICKSON, V. VERSHKOV[6], S. VON GOELER, F. WAGNER[10], R. WIELAND, J.B. WILGEN[1], M. WILLIAMS, K.L. WONG, S. YOSHIKAWA, R. YOSHINO[11], K.M. YOUNG, M.C. ZARNSTORFF, V.S. ZAVERYAEV[6], S.J. ZWEBEN

Princeton Plasma Physics Laboratory,
Princeton University,
Princeton, New Jersey,
United States of America

Abstract

TFTR PLASMA REGIMES.

Significant extensions in the TFTR plasma operating regimes have been achieved with additional heating system capability, installation of a multishot pellet injector, and the development of an enhanced confinement regime. In ohmically heated pellet-fuelled discharges characterized by highly peaked

[1] Oak Ridge National Laboratory, Oak Ridge, TN, USA.
[2] University of Wisconsin, Madison, WI, USA.
[3] GA Technologies, Inc., San Diego, CA, USA.
[4] RCA David Sarnoff Research Centre, Princeton, NJ, USA.
[5] Balliol College, University of Oxford, Oxford, UK.
[6] Kurchatov Institute of Atomic Energy, Moscow, USSR.
[7] EG&G Idaho, Inc., Idaho Falls, ID, USA.
[8] JET Joint Undertaking, Abingdon, Oxfordshire, UK.
[9] University of Maryland, College Park, MD, USA.
[10] Max-Planck-Institut für Plasmaphysik, Garching, Fed. Rep. Germany.
[11] JAERI, Naka-machi, Naka-gun, Ibaraki-ken, Japan.

density profiles, enhancements in τ_E have resulted in $n_e(0)\tau_E(a)$ values of 1.5×10^{20} m^{-3}·s. In neutral beam heated discharges, an operating regime has been developed in which substantial improvements in energy confinement time and neutron source strength are observed. Ion temperatures of about 20 keV and $n_e(0)\tau_E(a)T_i(0)$ values of 2×10^{20} m^{-3}·s·keV have been achieved. This enhanced confinement regime is characterized by high values of β_p and low values of collisionality. The observed surface voltage, which is negative during beam injection, is compared with models including beam driven and bootstrap currents.

I. Introduction

The goals of the TFTR project are (1) to study reactor-grade plasmas with temperatures of order 10 keV and densities of order 10^{20} m^{-3}, and (2) to achieve approximate breakeven between the power input to and the fusion output from the plasma ($Q \sim 1$). During the past year, high-power neutral-beam-heating experiments and ohmic-heating experiments utilizing a deuterium pellet injector have significantly extended the operating regimes of TFTR, as measured by the $n_e(0)\tau_E(a)T_i(0)$ product and the Q-value achieved in neutral-beam-heated discharges.

This paper gives a brief description of the TFTR device status and the operating regimes in gas-fueled and pellet-fueled ohmic discharges. A more extensive discussion of the pellet-fueled discharges is given by Schmidt et al. [1]. Results from neutral-beam-heating experiments in the standard regime are also summarized briefly. A general description is given of the operating characteristics of discharges in the enhanced confinement regime; further information is contained in the papers by Goldston et al.[2], McGuire et al.[3], and Hill et al. [4].

II. Machine Status

An initial series of experiments with two (co-injecting) neutral beamlines was completed in April 1985, during which TFTR reached its original machine design specifications for plasma current and toroidal field (I_p = 2.5 MA and B_T = 5.2 T) [5]. Subsequently, two additional beamlines were installed; three beamlines are now aimed tangentially in the direction of the plasma current (co-injection), and one opposite (counter-injection). During the recent experiments, the maximum injected power was 20 MW with a full energy component of ~ 10 MW. The maximum beam voltage was 110 kV and the maximum pulse duration 1.0 s. Most of the experiments were conducted with 0.5 s pulse lengths and an average beam voltage of ~ 95 keV. Deuterium injection was used in all of the experiments discussed here. During the last beamline installation, a large-area axisymmetric inner wall limiter was also installed. This limiter is composed of water-cooled Inconel plates covered with graphite tiles. The toroidal inner wall limiter and moveable limiter define the present maximum plasma dimensions as $R \approx 2.48$ m and $a \approx 0.82$ m.

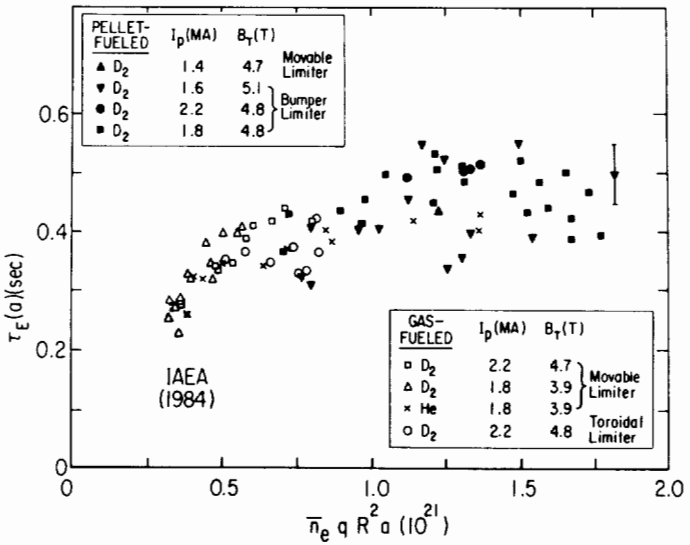

FIG. 1. Gross energy confinement versus $\bar{n}_e q_a R^2 a$ for ohmically heated discharges with and without pellet injection. The 1.6 MA discharges had reduced aperture, a = 0.7 m, compared with the other full-size 0.8 m discharges.

III. Ohmically Heated Discharges

Initial ohmic experiments reported in 1984 [6] at modest toroidal fields (≤ 2.8 T), plasma currents (≤ 1.4 MA), and densities ($\bar{n}_e < 3 \times 10^{19}$ m^{-3}) demonstrated that the global energy confinement time, τ_E, scales consistent with $\bar{n}_e q R^2 a$, reaching a maximum value of $\tau_E \sim 0.3$ s. Subsequent experiments utilizing both gas- and pellet-fueled discharges have concentrated on exploring the applicability of this scaling law over a wider operating range in density, toroidal field, and plasma current.

The analysis of the energy confinement time has relied principally upon a time-independent kinetic analysis code, SNAP, [5] and has been supplemented by magnetic measurements [7]. Figure 1 is a summary of the ohmic-heating studies for full bore plasmas. In gas-fueled deuterium discharges, the confinement time increases up to 0.44 s, in reasonable agreement with $n_e q_a$ scaling for $\bar{n}_e \lesssim 4.8 \times 10^{19}$ m^{-3}. At higher densities, saturation is found to occur for both helium-gas and deuterium-pellet fueled discharges. In the high density regime, the confinement time is observed to be a weak function of plasma current.

In addition to increasing the line-averaged density, pellet injection produces highly peaked density profiles. A line-averaged density of 1.4×10^{20} m^{-3} has been achieved 200 ms after the injection of five 2.7 mm pellets in experiments conducted on

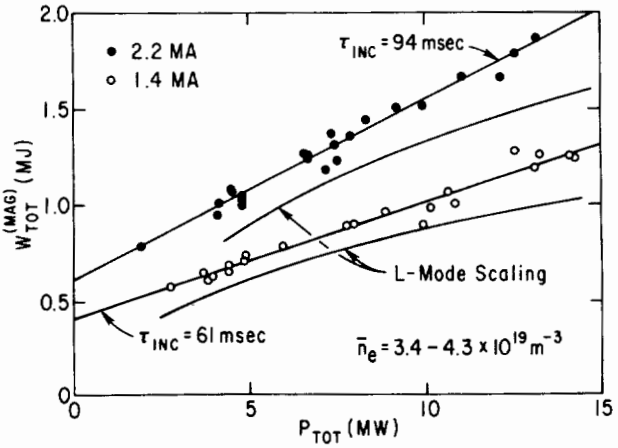

FIG. 2. Variation of the stored energy for 1.4 and 2.2 MA power scans, for a constrained density range and B_T = 4.8 T, R = 2.48 m, a = 0.82 m. Magnetic measurements are compared with prediction of the Goldston L-mode model.

the inner graphite limiter. This corresponds to a Murakami parameter, $\bar{n}_e R/B_T = 6.5 \times 10^{19}$ m^{-2} T^{-1}. The central electron density was 2.8×10^{20} m^{-3} and central electron temperature was 1.4 keV, as measured by Thomson scattering. This peaked density profile was achieved by operating with a reduced plasma minor radius of 0.7 m and a plasma current of 1.6 MA, in order to improve pellet penetration. The energy confinement time was ~0.50 s according to kinetic and diamagnetic measurements corresponding to an $n_e(0)\tau_E \simeq 1.4 \times 10^{20}$ m^{-3}·s. The energy confinement time is ~ 20% greater than that achieved in gas-fueled discharges with the same values of I_p, R, and a, using either deuterium or helium as the working gas.

IV. Neutral-Beam-Heating Studies in the Standard Regime

The variation of energy confinement time with injection power up to ~ 15 MW was studied systematically. These experiments were conducted in the large plasma configuration on the inner wall limiter with deuterium gas fueling, deuterium beams, I_p = 1.4 and 2.2 MA, and B_T = 4.8 T [7]. Figure 2 shows the variation in the total stored energy for the 1.4 and 2.2 MA power scan with a constraint on the density at the end of injection. Kinetic and magnetic measurements (using the techniques described in Ref. 7) are in good agreement. The stored energy increases linearly with heating power; however, the rate of increase of stored energy, dW_p/dP_{heat}, is appreciably less than the ohmic confinement time. The gross energy confinement time $\tau_E(a)$, defined as $W_{TOT}/(P_{TOT} - dW_{TOT}/dt)$, where $W_{TOT} = W_e + W_i + W_b$ and $P_{TOT} = P_{OH} + P_{INJ}$ for the data shown in Fig. 2, can be fitted to a form $\alpha + \beta/P_{TOT}$, where α is the "incremental" confinement time. In the plasma density

range of $3.4 < \bar{n}_e < 4.3 \times 10^{19}$ m^{-3}, α increases with plasma current from 61 ms to 94 ms as the current is increased from 1.4 to 2.2 MA. The energy confinement time is observed to depend weakly upon density; however, a negative scaling of α with increased density is observed in the 1.4 MA discharges. At low density, the enhancement in stored energy at high power occurs in the beam and thermal ions, since the electron stored energy decreases slowly with decreasing density. The high-power beam heating in this current and density range results are also in fair agreement with the Goldston L-mode model [8] for hydrogen injection into deuterium plasma. Power-law fits to the data shown in Fig. 2 indicate that $W_{TOT} \propto P_{TOT}^{0.46} I_p^{0.91}$ for $P_{TOT} > 4$ MW [7].

V. Neutral Beam Heating in the Enhanced-Confinement Regime

Previous operation of TFTR at low I_p (0.4-1.0 MA) and moderate beam power ($P_b < 6$ MW) using only co-injection [5] allowed access to a very low-density regime ($\bar{n}_e \sim 1 \times 10^{19}$ m^{-3}), characterized by high values of ion temperature (~ 9 keV) and rapid toroidal rotation velocity (up to ~ 7×10^5 m/s). Recent experiments in this regime conducted at higher power ($\lesssim$ 20 MW), using both co- and counter-injection, have demonstrated enhanced confinement relative to the predictions of L-mode scaling, along with central ion temperatures of ~ 20 keV at $\bar{n}_e \sim 3 \times 10^{19}$ m^{-3} with a central $n_e(0) \sim 7 \times 10^{19}$ m^{-3} [9]. The achievement of this improved performance relative to the previous experiments is due to extensive degassing of the limiter and near-balanced injection ($P_{ctr} \sim P_{CO}$).

A procedure that results in a low recycling rate, as shown by decreases in the D_α emission and edge neutral pressure, is identified to be critical in giving rise to the enhanced confinement regime [4,10]. Both low-density deuterium and helium discharges have been used to degas the inner wall. These high power discharges (0.8-1.8 MA) were not fueled following breakdown. Helium discharges were more effective in reducing the low-density limit and the decay time of the density following a diagnostic gas puff. The density decay time has been decreased from > 5 s to as low as ≈ 0.15 s after extensive degassing. The low initial density of the target plasma and relatively high Z_{eff} ~ 6 is a consequence of the degassing procedure which effectively removes D^+ from the target plasma. The large density rise during injection [$\bar{n}_e$(final)/$\bar{n}_e$(prior to injection) $\lesssim$ 3-4] is accompanied by a decrease in Z_{eff} to ~ 3 at the end of injection.

Figure 3 shows a comparison of the temporal evolution of two discharges during neutral beam injection with different initial line-integral densities, different deuterium recycling rates due to different degassing histories, and comparable final line-integral densities. In the discharge with the lower initial density, both the neutron source strength and the stored energy

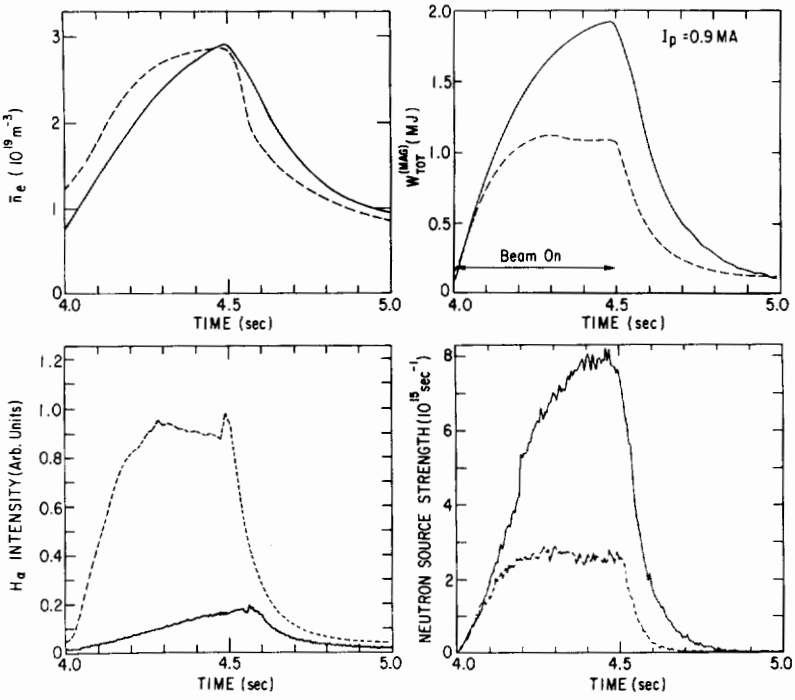

FIG. 3. Comparison of the evolution of line average density, neutron source strength, H_α emission (which includes both H_α and D_α emission) and stored energy for two discharges. The solid curve corresponds to a supershot. $R = 2.48$ m, $a = 0.82$ m, $P_b = 12.5$ MW and $B_T = 4.7$ T in the supershot discharge, whereas $P_b = 11.4$ MW and $B_T = 5.0$ T in the other shot.

increase throughout the 0.5 s neutral-beam pulse. The global energy confinement time is also substantially longer. Discharges that exhibit continually rising stored energy and neutron source strength during the half-second beam-injection have been colloquially termed "supershots". Experiments conducted in the final days of the experimental run demonstrated continued increase in stored energy with 0.7 s duration beam pulses and that the stored energy approached equilibrium with 1.0 s duration pulses. At plasma currents up to 1 MA, values of $\beta_p \simeq 2.0$ from plasma diamagnetism have been measured. Maximum values of β_p up to 2.2 have been achieved transiently. These high values of β_p result in substantial outward shifts of the magnetic axis $(R_{mag}-R_{geo})/a \lesssim 0.4$ and distortions of the plasma shape. The vertical elongation, κ, decreases from 1.05 to $\lesssim 0.9$ in the most extreme cases. Figure 4 shows a comparison of the electron temperature and density profiles measured near the end of the pulse for the discharges shown in Fig. 3. The discharge with the lower initial density (supershot) has a more peaked density profile, with a higher central density and a much broader electron temperature profile. Peak central electron temperatures of ~ 6.5 keV during injection have been obtained in supershots.

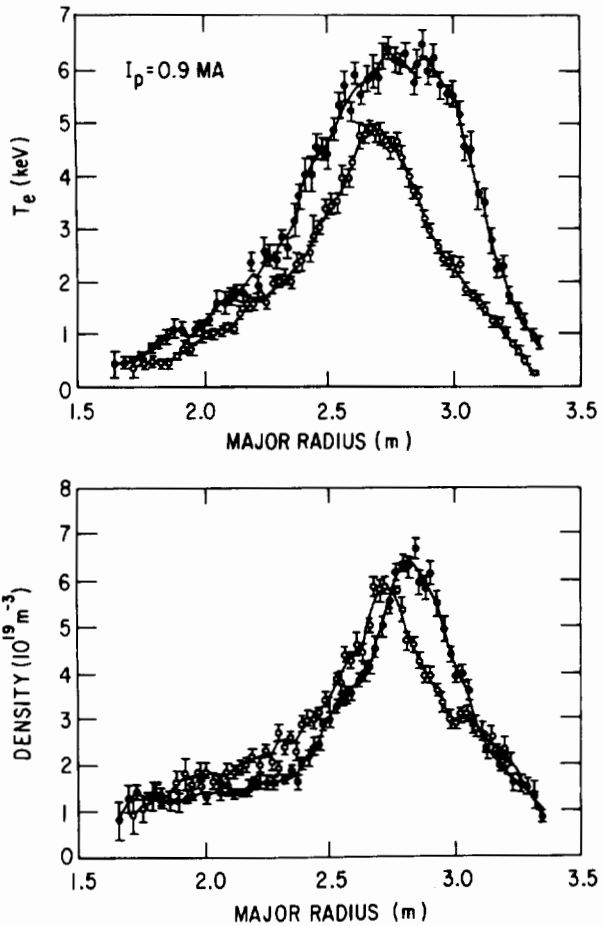

FIG. 4. Comparison of Thomson scattering measurements of the electron temperature and density profiles at 4.45 s for the discharges shown in Fig. 3. The solid points are for the supershot discharge and the open circles are for the other shot.

The central ion temperature is measured using several techniques. X-ray Doppler-broadening measurements have been carried out for Fe XXV and Ni XXVII K_α lines using a horizontally viewing crystal spectrometer and three vertically viewing spectrometers. The horizontal channel is rendered ineffective, due to neutron noise during supershots. In the analysis of the vertical detectors the large shift in magnetic axis needs to be taken into account. For the data shown in Fig. 5, the emitting region viewed by the vertical detector is ~ 0.2 m outside of the magnetic axis. Doppler-broadening measurements in the VUV have also been used to obtain central ion temperatures. The

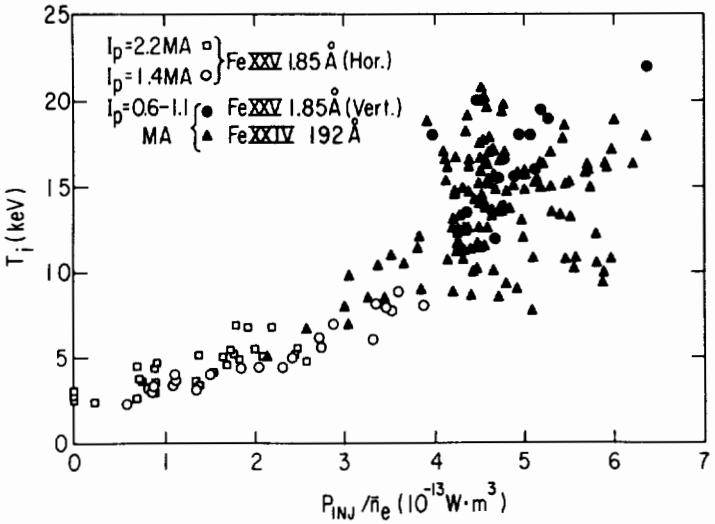

FIG. 5. Ion temperature versus $P_{INJ}/\bar{n}_e$. Closed symbols are for 4.8 < B_T < 5.2 T, 0.8 ≤ I_p ≤ 1.0 MA, R = 2.45 m and a = 0.80 m, and open symbols are for the discharges shown in Fig. 2.

spectrometer has a horizontal radial view of the plasma. One-dimensional impurity transport simulations including charge-exchange recombination indicate that the mean radius of the emission profile for the lithium-like ions used is ~ 0.2 m. The heating beams have permitted preliminary spectroscopic measurements utilizing carbon lines excited by charge-exchange recombination. Good agreement between the various measurements is achieved.

Figure 5 shows the variation in central ion temperature for discharges in the standard neutral-beam-heating regime (I_p = 1.4 and 2.2 MA) and for both super and non-super low-current discharges (0.6 < I_p < 1.1 MA). In the low-current discharges, considerable variability in the heating results is obtained, reflecting the occurrence of MHD activity, variations in limiter history, and variations in the fraction of power in the co-direction. Taking into account uncertainties in the measurements and the calculated differences between the impurity and hydrogenic ion temperatures which are < 2 keV, these results indicate central bulk ion temperatures of ~ 20 keV. The maximum value of the ion heating efficiency parameter, $\bar{n}_e \Delta T_i/P_{INJ}$, is ~ 3.8 x 10^{13} keV·W^{-1}·m^{-3}. This is in comparison with previous experiments [5] in which $\bar{n}_e \Delta T_i/P_{INJ}$ was ~ 1.5 x 10^{13} keV·W^{-1}·m^{-3}.

Figure 6 shows the scaling of stored energy with power. An important characteristic of the enhanced confinement regime is the fraction of power in the co-direction, P_{CO}/P_{INJ}. As shown in Fig. 6, at a given power the highest stored energy (and hence τ_E) is

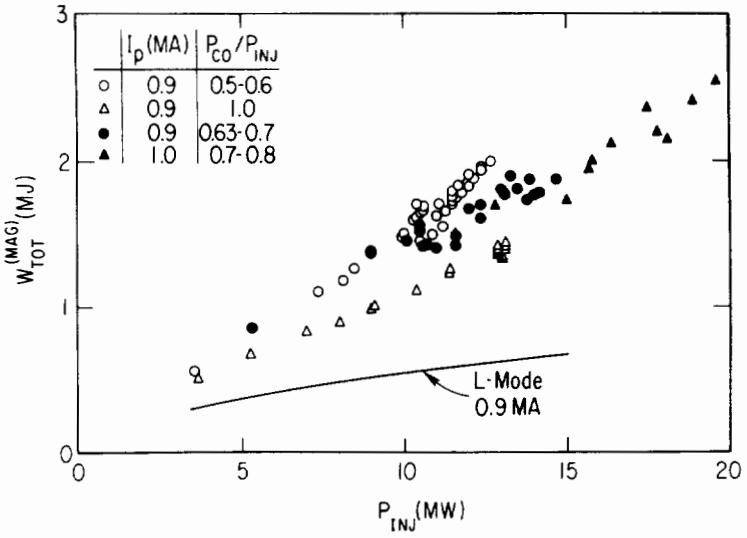

FIG. 6. Variation of stored energy with injected power for different values of fractional power in the co-direction, for 4.7 < B_T < 5.2 T, 2.40 < R < 2.48 m and 0.76 < a < 0.82 m. Magnetic measurements are compared with the prediction of the L-mode model of Goldston.

achieved with nearly balanced injection (P_{CO}/P_{INJ} ~ 0.5) in discharges with degassed limiters. In Fig. 6, the data set was constrained to eliminate discharges with very-large-amplitude continuous MHD activity [3]. With nearly balanced injection the stored energy increases linearly with heating power and the incremental confinement time is 0.15 s, comparable to the low-density ohmic confinement time prior to injection. Furthermore, with near balanced injection the global confinement time is not observed to degrade with power: values up to 0.17 s are achieved with 12 MW, as shown in Fig. 7, and the confinement time is up to ~ 3 times the prediction of Goldston L-mode scaling [8]. With the present distribution of beam sources, at full power P_{CO}/P_{INJ} is ≈ 0.7, which is not optimum, as indicated in Fig. 7. The highest power experiments were conducted at higher current (1.0 MA) to minimize the effects of MHD activity.

The energy stored in the discharge appears to be limited by a maximum β_p value of ~ 2. Further increases in power at a given current result in either disruptions or MHD activity degrading the stored energy [3]. At low toroidal field and modest q_a (~ 4-5), the maximum stored energy is in fair agreement with the Troyon β_T limit [$\beta_T^{max} \approx (2.2\text{-}2.5)\ \mu_o I_p/aB_T$] [11]. At high toroidal field and q_a the Troyon β_T limit would permit β_p values up to ~ 3.5.

At higher plasma current (I_p > 1.1 MA), the favorable characteristics of supershots have not been observed, and the

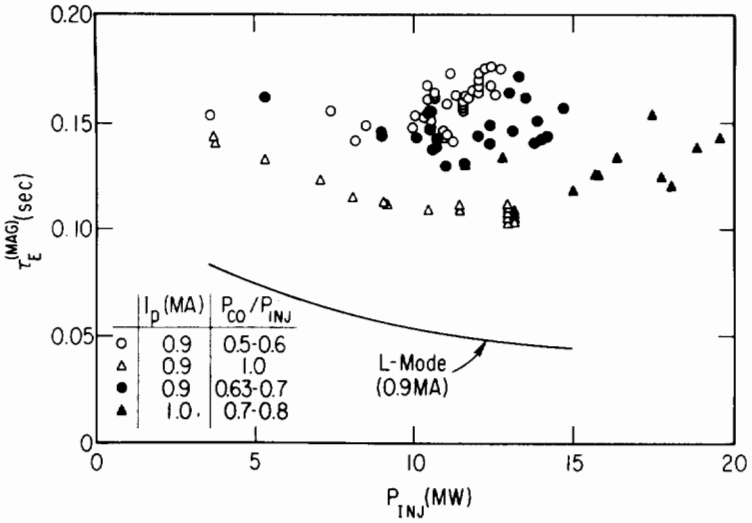

FIG. 7. Variation of global confinement time with injected power for the data set shown in Fig. 6. Magnetic measurements are compared with the prediction of the L-mode model of Goldston.

difference in τ_E between balanced and co-only injection at P_b = 10 MW is less than 15%. Supershot characteristics at higher current (1.3 MA with 17 MW of neutral beam power) can be achieved by ramping the current from 0.9 MA during the beam pulse, resulting in $q_a \approx 5$. Further extension of the operating regime may be possible with the longer-duration (2.0 s) and higher-full-energy-species-mix beam sources (80% power at full energy) that are currently being installed. Present current-ramp experiments are encouraging in that supershot characteristics are observed even when fairly large current-ramp rates up to 1 MA/sec are applied. By tailoring the beam power waveform and the current ramp, it may be possible to achieve supershots with much higher currents, thus avoiding the β limits.

In discharges in which the plasma current is maintained constant by feedback control, the surface voltage is observed to decrease from the ohmic phase with increasing β_p and co-injected power and is typically ~ -0.2 V at the end of injection. Though the electron temperature increases and broadens and Z_{eff} decreases, changes in conductivity alone cannot produce a negative voltage. The changes in plasma geometry coupled with changes in conductivity are also not large enough to account for the negative voltage, as determined by a one-and-one-half dimensional magnetic field diffusion calculation. Monte Carlo beam calculations show that neoclassical beam-driven currents [12] contribute to the decrease in surface voltage, but still do not account for the magnitude. The calculations show that, due to the beam orbits, co-injection is more effective in driving current, particularly in

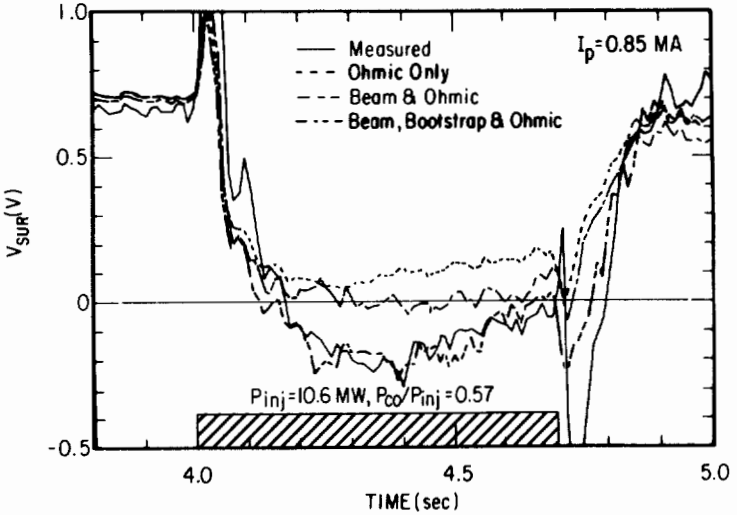

FIG. 8. Comparison of the measured surface voltage with the calculated surface voltage under different assumptions for the role of non-ohmically driven currents. The discharge parameters are B_T = 5.2 T, R = 2.45 m and a = 0.8 m.

outer regions of plasma, than counter-injection; thus, even when the power is nearly balanced, a net beam-driven current effect on the surface voltage is calculated. By including the neoclassical bootstrap current predicted by Galeev and Sagdeev [13] and Bickerton et al. [14] as formulated by Hirshman and Sigmar [12], good agreement is obtained between the calculated and measured surface voltage, as shown in Fig. 8. These calculations indicate that for this case approximately 350 kA of bootstrap current is present, compared with 420 kA of co-injected current and -160 kA of counter-injected current. In presently analyzed discharges, the maximum calculated bootstrap current is 440 kA in a 900 kA plasma with 370 kA of calculated beam-driven current. While the driven currents do not exceed the total current, the calculated voltage is negative because the radial distribution of the bootstrap current is broader than that of the ohmic current, exceeding the total current density in the outer region of the plasma.

Operation in the supershot regime has resulted in substantial increases in neutron source strength and equivalent Q. The maximum neutron source strength of 1.2 x 10^{16} n/s was achieved with 19.6 MW of beam power, with P_{CO}/P_{INJ} = 0.7. The maximum Q_{DD} of 8.7 x 10^{-4} was achieved with 12.3 MW, when the power was more nearly balanced ($P_{CO}/P_{INJ} \approx 0.56$), corresponding to a source strength of 8.9 x 10^{15} n/s. In the supershot regime, SNAP and time-dependent (TRANSP) calculations of the neutron flux are in good agreement (± 25%) with the measured flux. These calculations indicate that, for the discharge with the highest

value of Q_{DD}, ~ 17% of the flux is due to beam-beam reactions, ~ 53% due to beam-target, and ~ 30% from the thermalized ions shortly before the end of the beam pulse. In order to estimate the Q_{DT} which would be achieved with deuterium and tritium, it is necessary to assume a composition for the hydrogenic component of the target plasma. For the hypothetical condition of deuterium beam injection into a tritium plasma (with the same value of Z_{eff} = 3.3), Q_{DT} would be 0.23, due to beam-target reactions. Because beam fueling is clearly very important, a more realistic case would be to consider injection using deuterium and tritium beams into a 50%/50% deuterium/tritium plasma. In this case, the resulting value of Q_{DT} would be ≈ 0.18. A significant improvement over these values can be expected from the new long-pulse ion sources with better species mix, operation at 120 kV, and nearly balanced injection at full beam power, even without assuming higher injected power and improved plasma parameters.

VI. Summary

During the past year, substantial progress has been made in expanding the operating range of TFTR. Ohmically heated pellet-fueled discharges have resulted in exceptional central densities and $n_e(0)\ \tau_E(a)\ T_i(0)$ values of ~ 2 x 10^{20} $m^{-3} \cdot s \cdot keV$. Furthermore, in the saturated regime, the confinement time in pellet-fueled discharges is observed to be longer than that achieved in gas-fueled discharges. In these discharges, the density profile is very peaked, $n_e(0)/\bar{n}_e$ ~ 2.

In neutral-beam-heated discharges an enhanced confinement regime has been found. This regime is characterized by peaked density profiles, broad electron temperature profiles, high ion temperatures, ≈ 20 keV, and high neutron source strengths. In this regime, $n_e(0)\ \tau_E(a)\ T_i(0)$ values of ~ 2 x 10^{20} $m^{-3} \cdot s \cdot keV$ have also been achieved. The operating regime is characterized by a low initial density and deuterium recycling prior to injection, which can only be achieved at low I_p and after extensive limiter degassing. At high toroidal field (B_T = 5.2 T), this corresponds to relatively high values of q_a (in the range of 7-8) and β_p (up to 2). In reduced toroidal field experiments and in current ramp experiments, supershots with q_a ~ 4-5 have been obtained. Significantly improved performance is achieved with nearly balanced injection.

In the high temperature regime, the plasma collisionality is low and β_p is high, so that both beam-driven currents and bootstrap currents are predicted to be important. Calculations including bootstrap current are in better accord with the experimental measurements than those including only the beam-driven currents. If these indications of the bootstrap current are verified by future experiments, the performance of tokamak reactors could be fundamentally enhanced.

Acknowledgements

We are grateful to D.J. Grove and J.R. Thompson for their advice and support, and to J. Strachan for his many contributions. This work was supported by US DOE Contract No. DE-AC02-76CH03073. The ORNL participants were also supported by US DOE Contract No. DE-AC05-84OR21400 with Martin Marietta Energy Systems, Inc.

REFERENCES

[1] SCHMIDT, G., et al., Paper IAEA-CN-47/A-III-4, these Proceedings, Vol. 1.
[2] GOLDSTON, R.J., et al., Paper IAEA-CN-47/A-II-1, these Proceedings, Vol. 1.
[3] McGUIRE, K., et al., Paper IAEA-CN-47/A-VII-4, these Proceedings, Vol. 1.
[4] HILL, K.W., et al., Paper IAEA-CN-47/A-IV-2, these Proceedings, Vol. 1.
[5] MURAKAMI, M., et al., Plasma Phys. Controll. Fusion **28** (1986) 17.
[6] EFTHIMION, P.C., et al., in Plasma Physics and Controlled Nuclear Fusion Research 1984 (Proc. 10th Int. Conf. London, 1984), Vol. 1, IAEA, Vienna (1985) 29.
[7] BELL, M.G., et al., Plasma Phys. Controll. Fusion **28** (1986) 1329.
[8] GOLDSTON, R.J., Plasma Phys. Controll. Fusion **26** (1984) 87.
[9] STRACHAN, J.D., et al., submitted to Phys. Rev. Lett., 1986.
[10] DYLLA, H.F., et al., submitted to Nucl. Fusion, 1986.
[11] TROYON, F., et al., Plasma Phys. Controll. Fusion **26** (1984) 209.
[12] HIRSHMAN, S.P., SIGMAR, D.J., Nucl. Fusion **21** (1981) 1079.
[13] GALEEV, A.A., SAGDEEV, R.Z., Zh. Ehksp. Teor. Fiz. **53** (1967) 348 (Sov. Phys. — JETP **26** (1968) 233).
[14] BICKERTON, R.J., CONNER, J.W., TAYLOR, J.B., Nat. Phys. Sci. **229** (1971) 110.

DISCUSSION

A. GIBSON: In the two cases for which you quote the large values of $\bar{n}_e \tau_E \bar{T}_i$, what is the ratio $\bar{n}_D/\bar{n}_e$?

R.J. HAWRYLUK: In high density pellet fuelled discharges, the correction factor for depletion is small, since Z_{eff} is about one. In the supershot discharge, the depletion factor, $n_D(0)/n_e(0)$, is about 0.7.

M. GREENWALD: Are you quite sure of the Z_{eff} profiles in your pellet fuelled shots? I ask this because there seems to be evidence of impurity accumulation.

R.J. HAWRYLUK: We do not have Z_{eff} profile measurements for the pellet fuelled discharges. In some discharges, there is substantial radiation on axis; however, even small concentrations of impurities would be adequate to explain the power loss.

Further, experiments are required to analyse impurity transport in pellet fuelled discharges and to determine whether accumulation occurs and, if so, under what conditions.

S. ITOH: I would like to ask about the target plasma for the 'supershot'. Is the target plasma in a slide-away regime? Judging by the target parameters, it would seem to be. Secondly, did you see any input power limit or threshold for the injection? The supershot discharges seem to be similar to the ASDEX discharges with slide-away electrons reported at the 1982 Conference.

R.J. HAWRYLUK: In some of the target plasma, electron cyclotron emission measurements indicate the presence of slide-away electrons. However, they are not evident in all of the supershot discharges and the occurrence of a slide-away does not appear to be a critical parameter.

Regarding your second question, at a given current there is an upper power limit present that corresponds to attainment of the β_p limit ($\beta_p \sim 2$) which I discussed. However, higher current operation enables us to inject the available 20 MW of neutral beam power and to maintain supershot characteristics.

K. LACKNER: Troyon-type scalings, $\beta_{pol,\,crit} \sim q_0$, are obtained for current density profiles adjusted to maintain q on axis at a constant value of about one. A reduction in $\beta_{pol,\,crit}$ and independence of it from q_a, as reported by you for low currents, would follow from theory for a current density profile flatter and non-dependent on q_a.

R.J. HAWRYLUK: In their paper, McGuire and co-workers* show that the profiles are not optimal, which is why the experimental beta limit is below that predicted by Troyon. The lack of sawteeth indicates that q on axis is greater than one. However, since the current penetration time is long compared with the beam duration, q is not substantially greater than one, according to our analysis.

M. BRUSATI: You have reported degradation of performance correlated with enhanced MHD activity. Can you comment on the kind of MHD spectra that you get?

R.J. HAWRYLUK: The mode number of the continuous MHD activity which degrades performance is typically m/n = 2/1 or 3/2. For further details, I would refer you to the paper by McGuire and co-workers that I have just mentioned.*

* Paper IAEA-CN-47/A-VII-4, these Proceedings, Vol. 1.